

SUPPLEMENTARY TABLE

Table S1. Differential ATAC-seq peaks with increased chromatin accessibility in EpiSCs grew in curved niche is preferentially associated with gene upregulation.

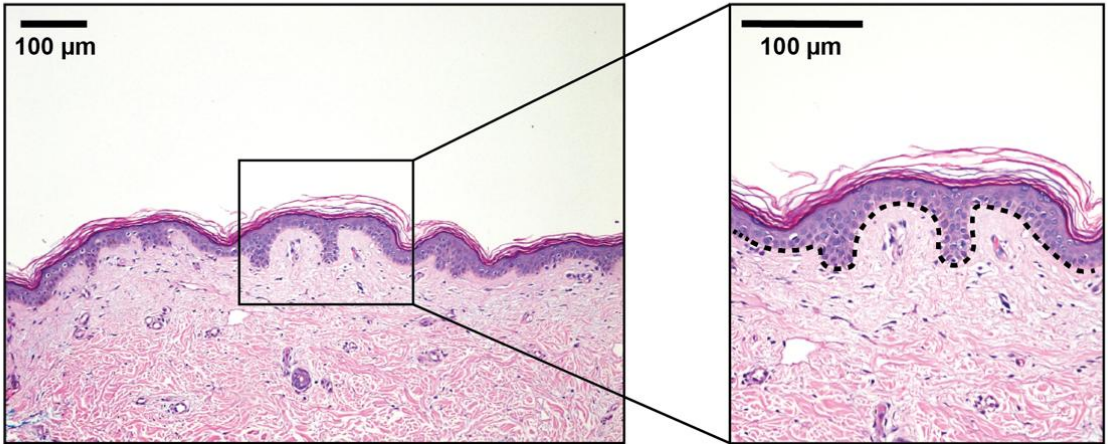
| | ATAC Differential Peaks | | ATAC Differential Peaks | |
|--------------------------------------|-------------------------|---------------|-----------------------------|---------------|
| | FRD<0.05 FC >=1.5 | | nominal p<0.05 FC >=1.5 | |
| | curved < flat | curved > flat | curved < flat | curved > flat |
| No. associated Genes # | 2540 | 112 | 6160 | 1999 |
| No. associated DEGup | 171 | 10 | 393 | 180 |
| No. associated DEGdown | 149 | 2 | 389 | 115 |
| ratio ass_DEG_up/ass_DEG_down | 1.15 | 5.00 | 1.01 | 1.57 |
| Fisher exact test pvalue | 0.24 | 0.039 | 0.09 | 0.006 |
| Chi-square test pvalue | 0.219 | 0.021 | 0.886 | 1.50E-04 |
| normalized ass_DEG ratio * | 0.96 | 4.17 | 0.84 | 1.30 |
| Fisher exact test pvalue | 0.672 | 0.077 | 0.003 | 0.0173 |
| Chi-square test pvalue | 0.661 | 0.045 | 0.0028 | 0.017 |

#, within 5kb to transcription start sites (TSS+/-5kb)

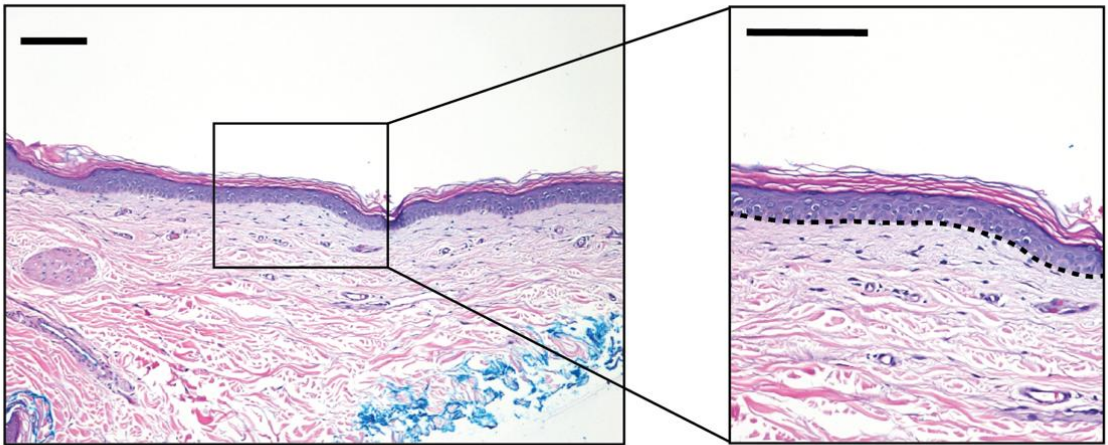
*, DEGup = 1,242, DEGdown = 1,034, Ratio (up/down) = 1.2

Supplementary Figure S1.

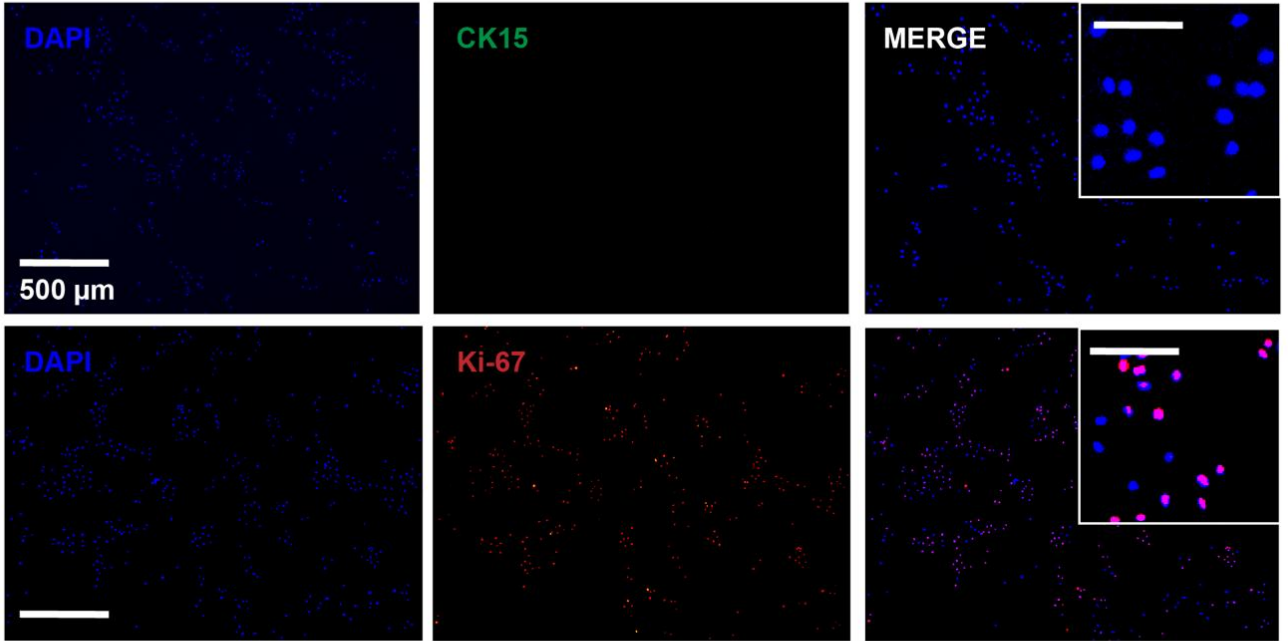
A



B



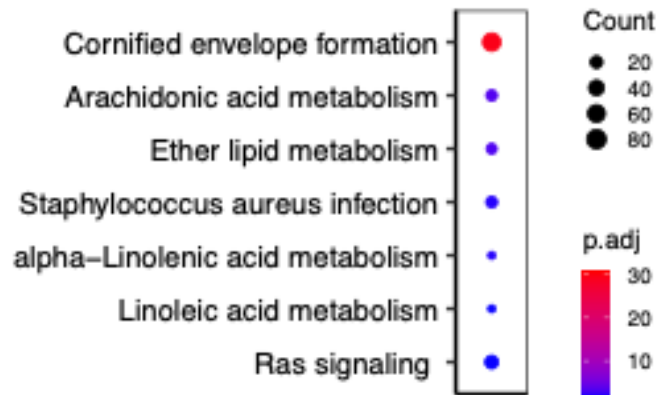
Supplementary Figure 3.



Supplementary Figure 4.

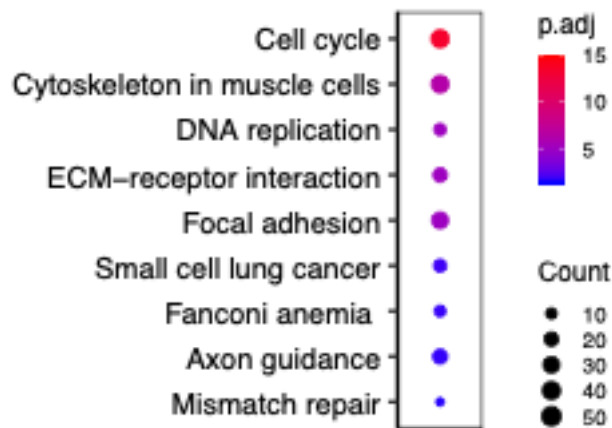
A

KEGG enrichment: upregulated genes in EpiSCs in curved niche



B

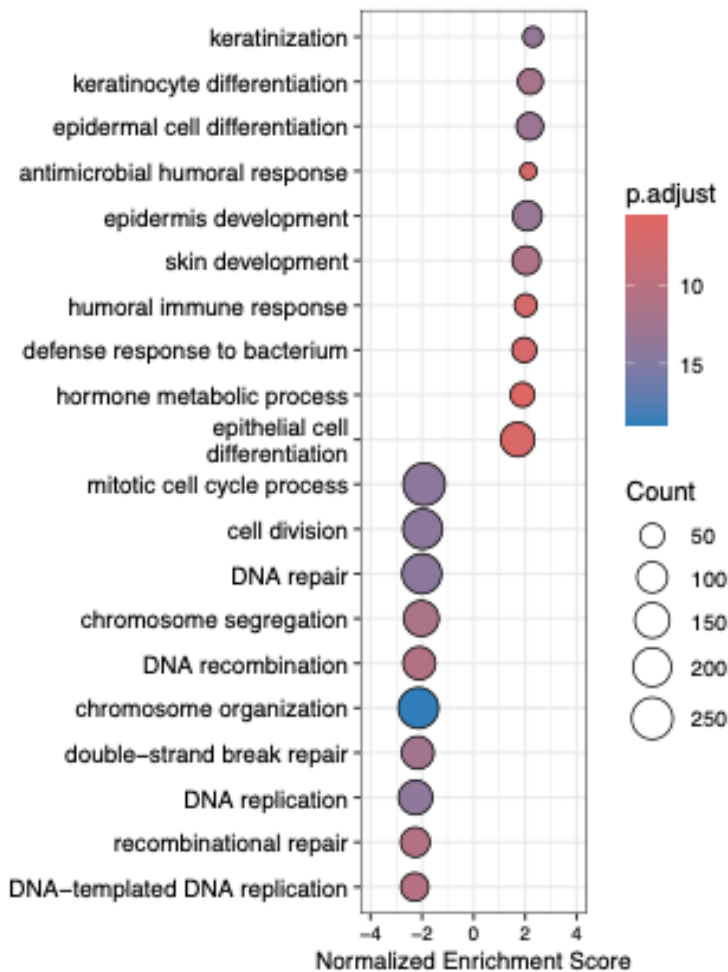
KEGG enrichment: downregulated genes in EpiSCs in curved niche



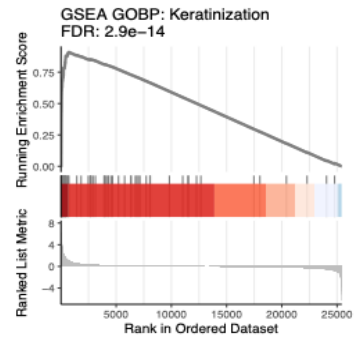
Supplementary Figure 5.

A

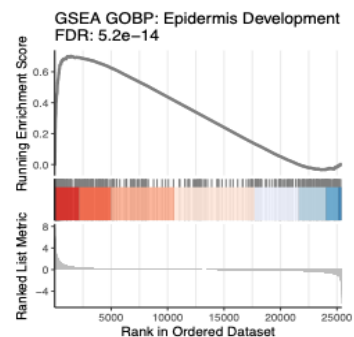
GSEA: Top 10 up- and down-regulated GOBP pathways



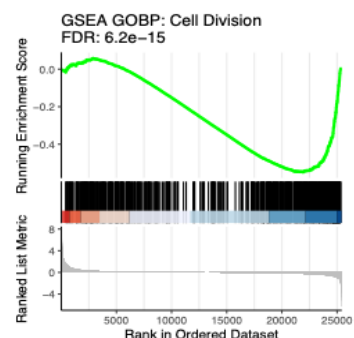
B



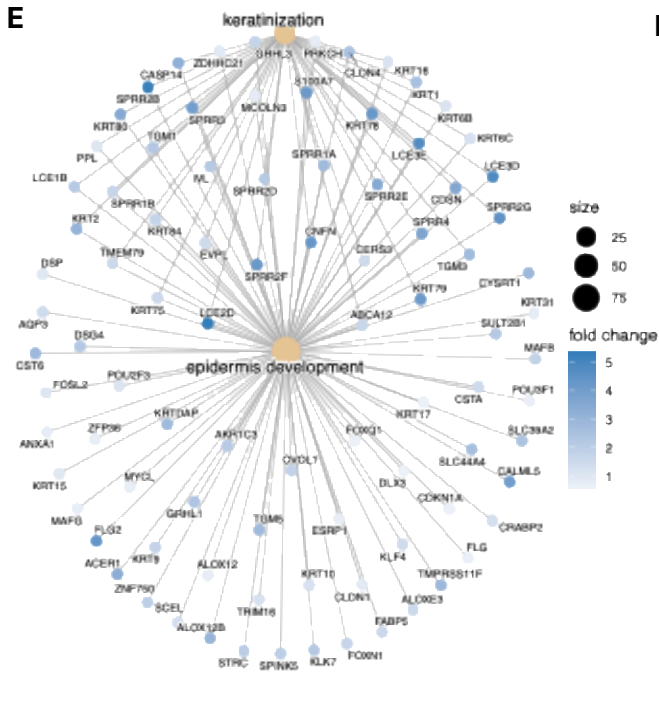
C



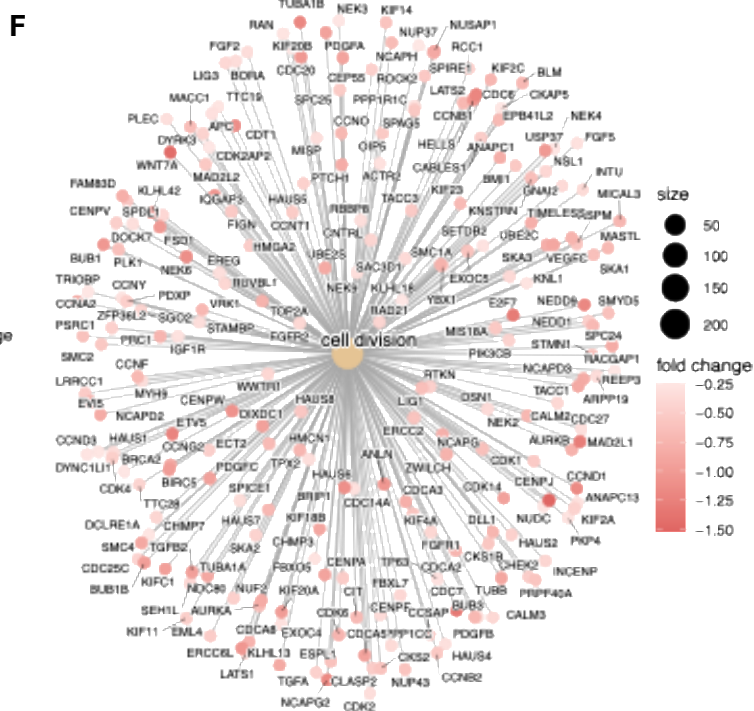
D



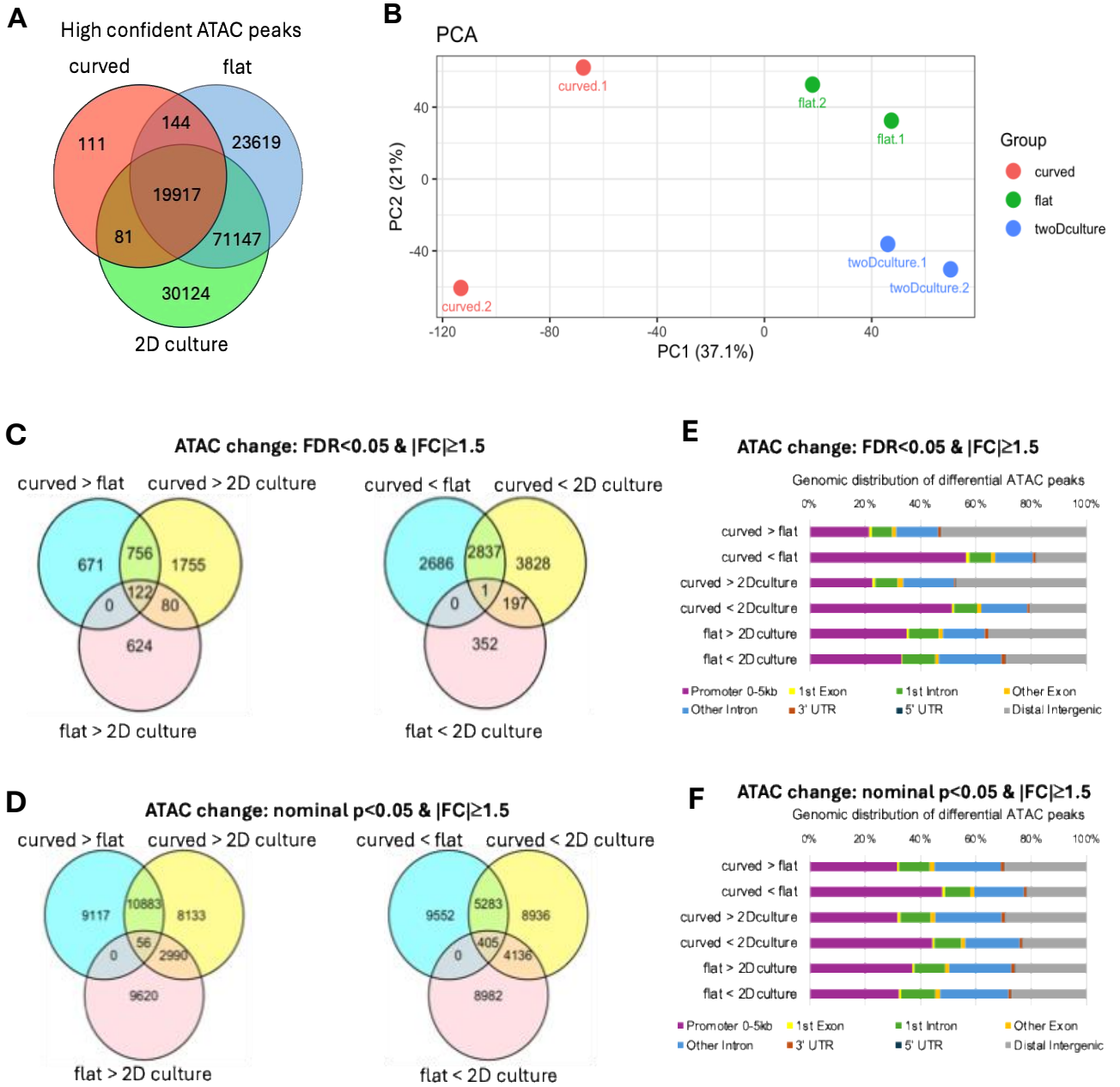
E



F

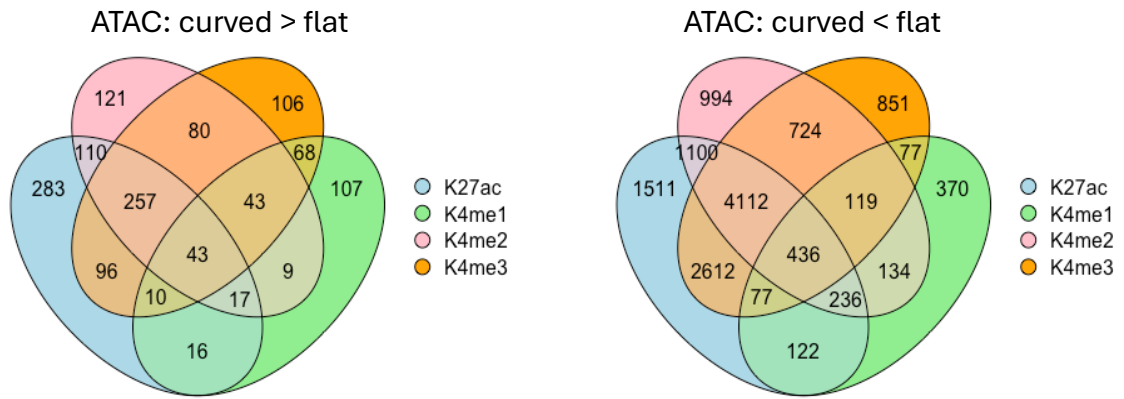


Supplementary Figure 6.

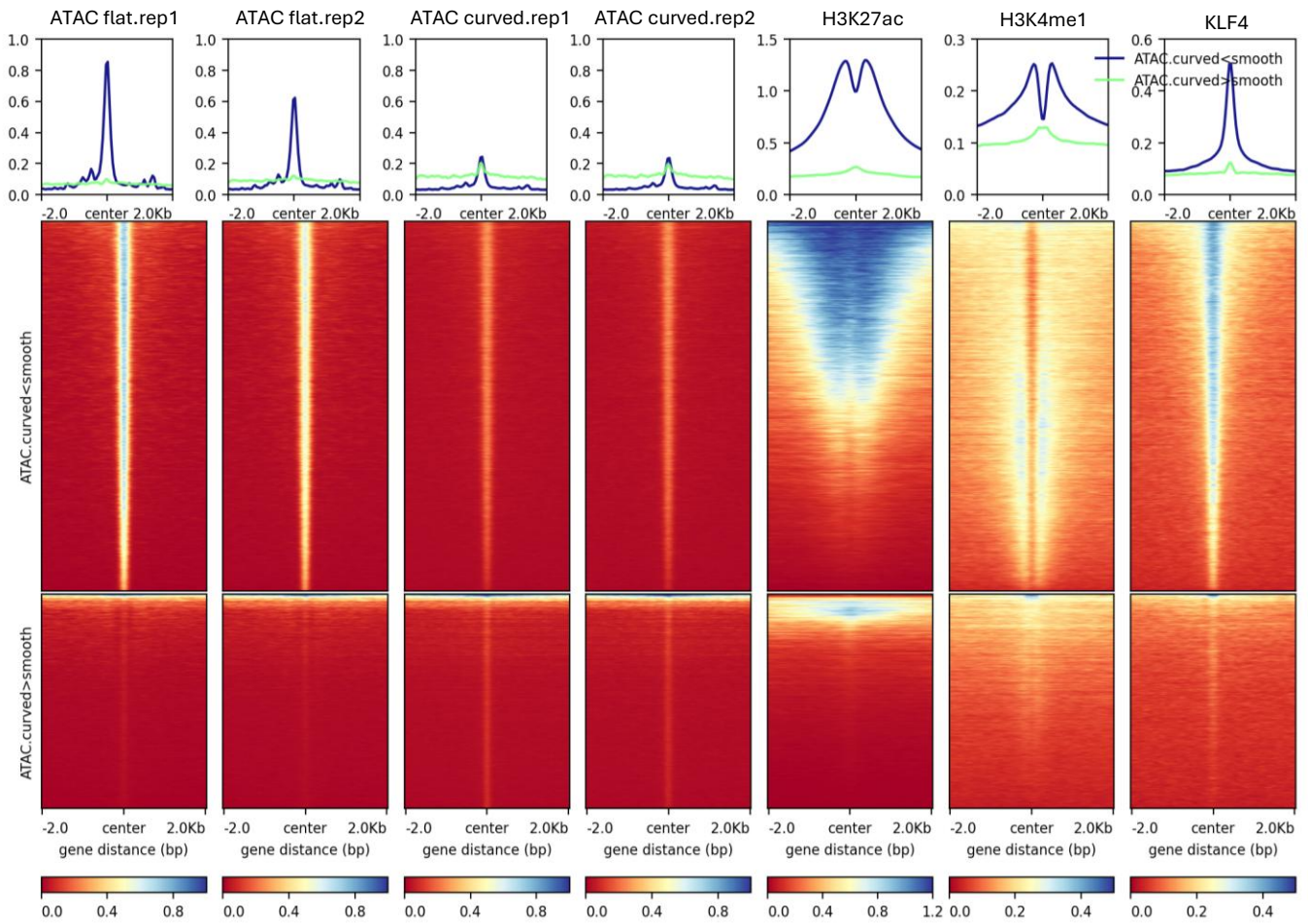


Supplementary Figure 7.

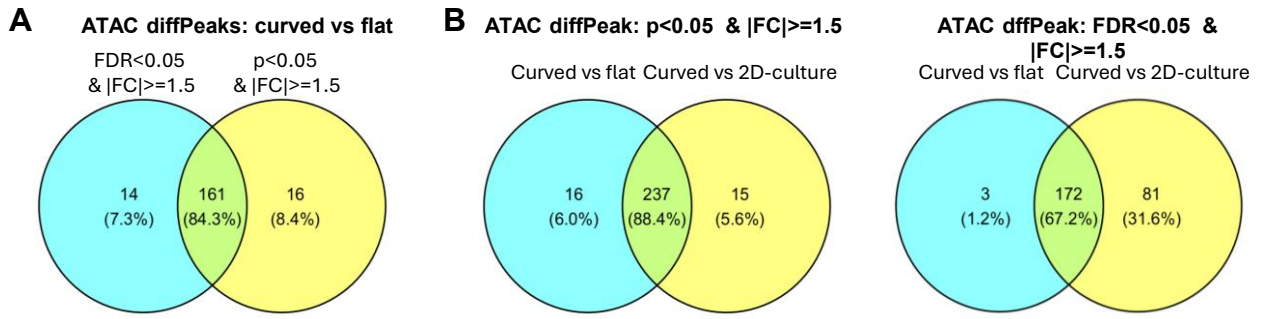
A Overlaps of differential ATAC regions with histone peaks



B

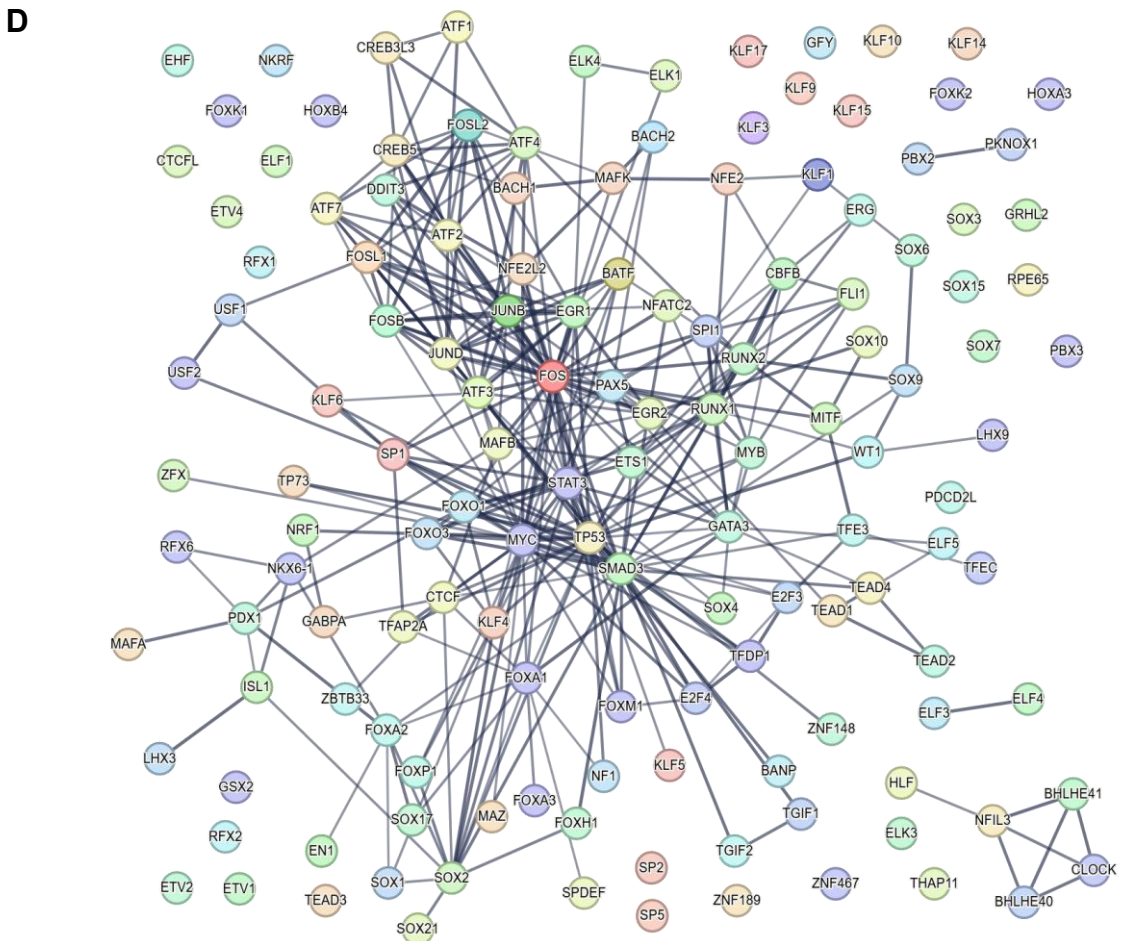


Supplementary Figure 8.



C

| Motif Name | Consensus sequence | Comparison | ATAC differential peaks: p < 0.05, FC > 1.5 | | ATAC differential peaks: FDR < 0.05 & FC ≥ 1.5 | |
|------------|--------------------|----------------------|---|----------------------|--|----------------------|
| | | | -log(Pvalue) | No. sites with motif | -log(Pvalue) | No. sites with motif |
| KLF4 | | curved vs flat | 655.7 | 2906 | 290 | 782 |
| | | curved vs 2D-culture | 555.6 | 3179 | 263 | 943 |
| | | flat vs 2D-culture | 278.3 | 1780 | 18 | 88 |
| SOX9 | | curved vs flat | 49.2 | 2172 | 17 | 422 |
| | | curved vs 2D-culture | 52.2 | 2550 | 13 | 549 |
| | | flat vs 2D-culture | 24.8 | 1685 | n.s. | — |



SUPPLEMENTARY FIGURE LEGENDS

Figure S1. Representative Hematoxylin and eosin (H&E) staining of young skin and aged skin. Prominent rete ridge architecture with pronounced epidermal invaginations were observed in young skin (A), whereas aged skin exhibits characteristic epidermal atrophy and loss of rete ridge architecture (B).

Figure S2. Optimization of keratinocyte culture and cell seeding on engineered curved and flat scaffolds. A. Representative phase-contrast images of primary keratinocytes cultured under standard 2D cell culture conditions showing cell morphology and proliferation at passage 1 (P1) on day 1, day 3, and day 4 after plating. B. Live/Dead Viability/Cytotoxicity assay demonstrates robust cell survival following culture on the scaffold system. Live cells were marked by green-fluorescent calcein-AM; dead cells were marked by red-fluorescent ethidium homodimer-1. The merged image shows the predominance of viable cells. The inset highlights representative live cells at higher magnification. C. Representative phase-contrast images of keratinocytes seeded onto rete ridge-patterned scaffolds compared with flat control matrices. At 0 h, cells are evenly distributed across both surfaces. At 36 h post-seeding, cells preferentially localize within the concave regions of the engineered rete ridge structures (dashed circles), while cells on flat matrices display a uniform distribution. These observations demonstrate that the engineered topography promotes preferential cell occupancy within niche-like concave microenvironments.

Figure S3. Validation of epidermal stem cell and differentiation markers in keratinocytes cultured under conventional 2D conditions. Representative immunofluorescence staining of keratinocytes cultured on flat substrates showing the expression of markers associated with distinct stages of epidermal lineage progression. Nuclei are counterstained with DAPI (blue). CK15 staining shows minimal or absent signal under these culture conditions. Ki-67 (red) marks proliferating cells, indicating active cell cycling within the keratinocyte population. FABP5 (red) identifies cells associated with transit-amplifying or early differentiation states, while involucrin (IVL) (red), a precursor of the cornified envelope, marks late-stage keratinocyte differentiation. Merged images show co-localization with nuclear staining, and insets display higher-magnification views of representative cells. Scale bars, 500 μm , unless otherwise indicated.

Figure S4. KEGG pathway enrichment of differentially expressed genes in EpiSCs cultured in curved niche versus flat scaffold. A. Pathways enriched among upregulated genes. B. Pathways enriched among downregulated genes.

Figure S5. Gene Set Enrichment Analysis (GSEA) of ranked gene expression changes in EpiSCs in curved niche versus flat scaffold. A. Dotplot of top 10 upregulated and top 10 downregulated GOBP pathways. B-D. GSEA enriched plots of GOBP pathways including Keratinization (B), Epidermis Development (C), and Cell Cycle (D). E-F. CNET plots of selected GOBP pathways. Most genes related to keratinization and epidermis development were upregulated (E, blue), while most genes related to cell division were downregulated (F, red).

Figure S6. Chromatin accessibility changes in EpiSCs cultured in a 3D curved niche, on a flat scaffold, or in standard 2D culture. A. Venn diagram of ATAC-seq peaks identified in EpiSCs cultured in a curved niche, on a flat scaffold, or in standard 2D culture. Biological replicates were used in MACS2 narrow peak calling to define consensus peaks. B. Principal component analysis of read counts at merged ATAC-seq peaks (combining all peaks identified in either replicate of the three conditions) shows clear separation among curved, flat, and 2D culture samples. C–D Venn diagrams comparing differential ATAC-seq peaks identified using two significance thresholds. E–F Genomic distribution of differential ATAC-seq peaks identified using the same thresholds. For panels (C, E), $FDR < 0.05$ and $\text{fold change} \geq 1.5$; for panels (D, F), nominal $p < 0.05$ and $\text{fold change} \geq 1.5$.

Figure S7. Histone modification landscape at differential ATAC-seq regions in EpiSCs cultured in a curved niche. A. Venn diagram showing the overlap between differential ATAC-seq regions (with increased or decreased accessibility) and active histone marks (H3K27ac, H3K4me1, H3K4me2, and H3K4me3) identified in keratinocytes. B. Heatmap of histone modification and transcription factor ChIP-seq signals in keratinocytes flanking differential ATAC-seq regions.

Figure S8. HOMER motif enrichment analysis at differential ATAC-seq peaks. A-B. Venn diagram of motifs enriched in differential ATAC peaks comparing EpiSCs grown in curved niche versus flat scaffold (A), and curved niche versus 2D-culture (B) using two selection criteria: $FDR < 0.05$ and $|FC| \geq 1.5$, or nominal $p < 0.05$ and $|FC| \geq 1.5$. C. Enrichment of KLF4 and SOX9 motifs. D. Protein-protein interaction network of transcription factors corresponding to motifs commonly enriched in curved vs. flat and curved vs. 2D culture differential ATAC peaks identified using both selection criteria. Motif enrichment was performed using HOMER. All motifs shown had $p.\text{adj} < 0.001$. Protein-protein interaction network was generated by STRING.